


RESEARCH ARTICLE

Neural correlates of dynamic changes in working memory performance during one night of sleep deprivation

Yuanqiang Zhu¹  | Yibin Xi¹ | Jinbo Sun² | Fan Guo¹ | Yongqiang Xu¹ | Ningbo Fei² | Xinxin Zhang² | Xuejuan Yang² | Hong Yin¹ | Wei Qin²

¹Department of Radiology, Xijing Hospital, The Fourth Military Medical University, Xi'an, Shaanxi, China

²Sleep and Neuroimage Group, School of Life Sciences and Technology, Xidian University, Xi'an, Shaanxi, China

Correspondence

Wei Qin, Sleep and Neuroimage Group, School of Life Sciences and Technology, Xidian University, Xi'an, Shaanxi 710126, China.
Email: wqin@xidian.edu.cn

Hong Yin, Department of Radiology, Xijing Hospital, Fourth Military Medical University, No. 127 West Changle Road, Xi'an, Shaanxi 710032, China.
Email: yinhong@fmmu.edu.cn

Funding information

National Natural Science Foundation of China, Grant/Award Numbers: 81571651, 81601474, 81801772; National Basic Research Program of China, Grant/Award Number: 2015CB856403; Key Research and Development Program of Shaanxi Province, Grant/Award Number: 2017ZDXM-SF-048

Abstract

Total sleep deprivation (TSD) is common in modern society leading to deterioration of multiple aspects of cognition. Dynamic interaction effect of circadian rhythmicity and homeostatic sleep pressure on sustained attention have been intensively investigated, while how this effect was represented on performance and cerebral responses to working memory, another important element of many neurobehavioral tasks, was not well elucidated. Thirty-six healthy subjects with intermediate chronotype performed the Sternberg working-memory task (SWMT) while undergoing functional magnetic resonance imaging every 2 hr from 10:00 p.m. on the first day to 6:00 a.m. on the second day. Using data from three imaging sessions (10:00 p.m., 04:00 a.m., and 06:00 a.m.), we found that the slowest SWMT reaction time and weakest cerebral responses were not at the end of TSD (06:00 a.m.) but during the early morning (04:00 a.m.) hours of the TSD. In addition, during this worst period of TSD, reaction time for the SWMT were found to be negatively correlated with task-related activation in the angular gyrus and positively correlated with the degree of negative correlation between the control and default networks. Our results revealed a rebound of SWMT reaction time and cerebral responses after the mid-time point of regular biological sleep night and provided more evidence that different cognitive tasks are differentially affected by sleep loss and circadian rhythmicity.

KEYWORDS

dynamic changes, rebound response, sleep deprivation, working memory

1 | INTRODUCTION

A single night of total sleep deprivation (TSD) produces a range of fundamental neurocognitive deficits and is associated with serious outcomes (Basner, Rao, Goel, & Dinges, 2013; Lim & Dinges, 2010). To understand the neural underpinnings of TSD-related deterioration within a specific cognitive domain, most imaging studies typically conduct two imaging sessions for each participant, one after TSD and the other after rested wakefulness (RW). The neurocognitive consequences of TSD were

largely explained by comparing the differences in brain activity between these two sessions (Durmer & Dinges, 2005; Goel, Rao, Durmer, & Dinges, 2009). However, these types of observations describe modulated cerebral responses rather than the process through which the modulation occurs. A recent study exploring 13 repeated functional magnetic resonance imaging (fMRI) sessions during 42 hr of TSD found differential results for cortical and subcortical responses during a psychomotor vigilance task (PVT) and greatly expanded our understanding of how sustained attention deteriorates during TSD (Muto et al., 2016). Thus, to better understand how sleep deprivation impairs cognitive performance, increasing the numbers of sessions and investigating dynamic changes in behavioral and cerebral responses is critical.

Yuanqiang Zhu, Yibin Xi, Jinbo Sun, Fan Guo authors contributed equally to this work.

Performance on the PVT and neuronal responses in high-order association cortex have both been found to gradually decrease as TSD progresses (Muto et al., 2016). Our recent study provided more detailed information about the process underlying PVT activation during one night of TSD, that is, for the fastest RTs, a compensatory increased activation was observed, followed by a rapid decreased activation in the late night of TSD; For the slowest RTs, gradually decreased segregation of the default mode network (DMN) from the task (increased DMN activation) was observed (Zhu et al., 2017).

However, how task performance and cerebral responses related to working memory (WM) are modulated during TSD is still not well understood (Mu et al., 2005a). WM is another important element of many neurobehavioral tasks, brain activity during a WM task typically involves widespread networks, including prefrontal regions, parietal regions as well as occipital lobe. The impact of SD on WM performance and its underlying cerebral correlates has repeatedly been investigated. Compared to RW condition, activity decreases have been extensively observed in fronto-parietal brain areas and were related to performance decline after SD (Habeck et al., 2004). Chee and Choo (2004) reported decreased parietal activation using two WM tasks, their further study indicated there were comparably reduced activations in bilateral superior parietal region at two test times (24 hr of SD and 35 hr of SD) when compared with RW (Chee et al., 2006). Furthermore, Chee and Choo (2004) and Lythe, Williams, Anderson, Libri, and Mehta (2012) indicated that the changes of frontal and parietal activity after SD were also dependent on task difficulty. Interestingly, cerebral task-related deactivation were also found to be closely related with performance impairment. However, as suggested by Reichert, Maire, Schmidt, and Cajochen (2016) it is important to note that the decreases in cerebral correlates do not only mirror an increase in sleep-pressure, but might be due the influence of the interaction of circadian and sleep-homeostatic factors.

Studies have indicated that sleep loss and circadian rhythmicity affect performance differently depending on the cognitive task (Schmidt, Fabienne, Christian, & Philippe, 2007). Supporting this, recent studies have indicated that the effect of sleep loss on WM tasks is smaller than the effect on sustained attention (Lo et al., 2012). Specifically, the maximum effects of circadian rhythmicity and sleep history on *n*-back WM were found at around 4 hr after dim light melatonin onset (DLMO+4 hr; Lo et al., 2012), which corresponds to the middle of the biological night (Klerman, Gershengorn, Duffy, & Kronauer, 2002). Therefore, cortical activity during WM tasks might also be affected differentially by interactions between homeostatic sleep pressure and circadian rhythmicity.

In the present study, we used repeated fMRI to investigate the changes in cerebral responses to the Sternberg working-memory task (SWMT) during a whole night of TSD (Cui et al., 2015; Mu, Mishory, et al., 2005a). As characteristics of the responses might be influenced by individual differences in sleep and wake preferences (known as chronotype; Roenneberg, Wirz-Justice, & Mellow, 2003), only subjects with intermediate chronotypes were recruited. We postulated that by scanning subjects repeatedly and evenly during TSD, we would be able to identify any dynamic changes in neuronal responses to the SWMT. Specifically, we hypothesized that (a) the worst performance and lowest levels of activation would be found at around the middle of biological

Significance Statement

Repeated fMRI was employed in our study to investigate the dynamic changes in performance and cerebral responses to Sternberg working-memory task (SWMT) during one night of total sleep deprivation (TSD). The slowest reaction time (RT) and weakest cerebral responses were found around the mid-time point of regular biological sleep (04:00 a.m.) which indicated a clear rebound at the end of TSD. These findings strengthen the fact that different cognitive task was differentially modulated by interactions between homeostatic sleep pressure and circadian rhythmicity. Previous TSD studies might miss critical information because the typical TSD condition occurs after the rebound of SWMT performance and response.

sleep night, (b) cerebral responses in Session 4 would be characterized by extensive deactivation, and (c) significant performance improvement and activation increase would be found in Session 5 compared with Session 4. To obtain further evidence for the functional relevance of activation patterns, we computed the correlation between SWMT performance and task-related cerebral responses in the different sessions.

2 | METHODS

2.1 | Participants

All research procedures were carried out in accordance with the Declaration of Helsinki and were approved by the Ethics Committee of Xijing Hospital, Fourth Military Medical University. All participants provided written informed consent prior to participation and were recruited from a group of college students. The basic recruitment criteria were similar to those that were used in our previous studies (Xu et al., 2015; Zhu et al., 2015). The inclusion criteria were as follows: (a) right-handed and (b) 18–35 years of age. The exclusion criteria were as follows: (a) a history of alcohol or drug abuse, (b) a present or past history of any psychiatric or neurological disorders according to the Structured Clinical Interview for Diagnostic and Statistical Manual of Mental Disorder-IV, (c) a history of sleep disorders according to International Classification of Sleep Disorders version 3 (Sateia, 2014), and (d) work that required shift hours. Individual chronotype was assessed by Munich Chronotype Questionnaire (MCTQ; Roenneberg et al., 2003; Roenneberg & Mellow, 2016), each participant was determined to be one of the seven potential types: extreme early, moderate early, light early, intermediate, light late, moderate late, and extreme late. The validity of MCTQ as a tool for chronotype classification has been verified by previous studies and is freely available at <http://www.thewep.org/chronotype-study>. Revised Chinese version of the MCTQ was used to classify the subjects (Chen et al., 2015). Hereby, Chronotype was estimated as the mid-sleep time on free days ($MSF = (\text{sleep onset on free day} + [\text{sleep duration on free day}]/2)$),

corrected for sleep debt on work days ($MSF_{SC} = MSF - [\text{sleep duration on free day} - \text{sleep duration on a working day}]/2$).

A total of 220 participants were screened for inclusion and exclusion criteria. Forty-five participants could not be included into the study as they did not meet the basic inclusion criteria, for example, history of alcohol disorders or sleep disorders, left handed. One hundred and thirty nine participants were excluded as they were not classified as intermediate chronotype. Hence, the final sample comprised 36 participants. Each person was provided a wrist actiwatch (Actiwatch; Philips Respironics; Mini Mitter, Bend, Oregon, USA) to monitor their sleep pattern (i.e., bed time, clock time falling asleep, clock time waking up, clock time getting up) 1 week before the fMRI experiment.

2.2 | Study procedure

Participants made two visits to the laboratory. During the first visit, they were briefed about the study protocol and were given an

actiwatch. A week later, they returned to the laboratory for the whole night of TSD. They were required to report to the laboratory no later than 6:00 p.m. on the test night, having stayed awake the whole day. First, high-resolution T1 MR images were obtained for each participant. All participants then performed the SWMT 10 times to exclude any effects related to practice. Consistent with previous studies, performance on this task showed a significant learning curve during the first five practices ($F[4,140] = 13.06, p < 0.001$), but reaching a stable level thereafter ($p > 0.2$, Figure 1c). Participants completed five SWMT sessions in the MR scanner, one every 2 hr, starting at 10:00 p.m. and ending at 6:00 a.m. (Session 1, 10:00 p.m.; Session 2, 12:00 a.m.; Session 3, 2:00 a.m.; Session 4, 4:00 a.m.; Session 5, 6:00 a.m.). Immediately after each scan, participants were instructed to complete 10 min of a PVT in the MR scanner. Following the PVT, they completed the Stanford sleepiness scale (SSS) by choosing one of seven statements that best described their current state of alertness. For the remaining time until the next scan, they were

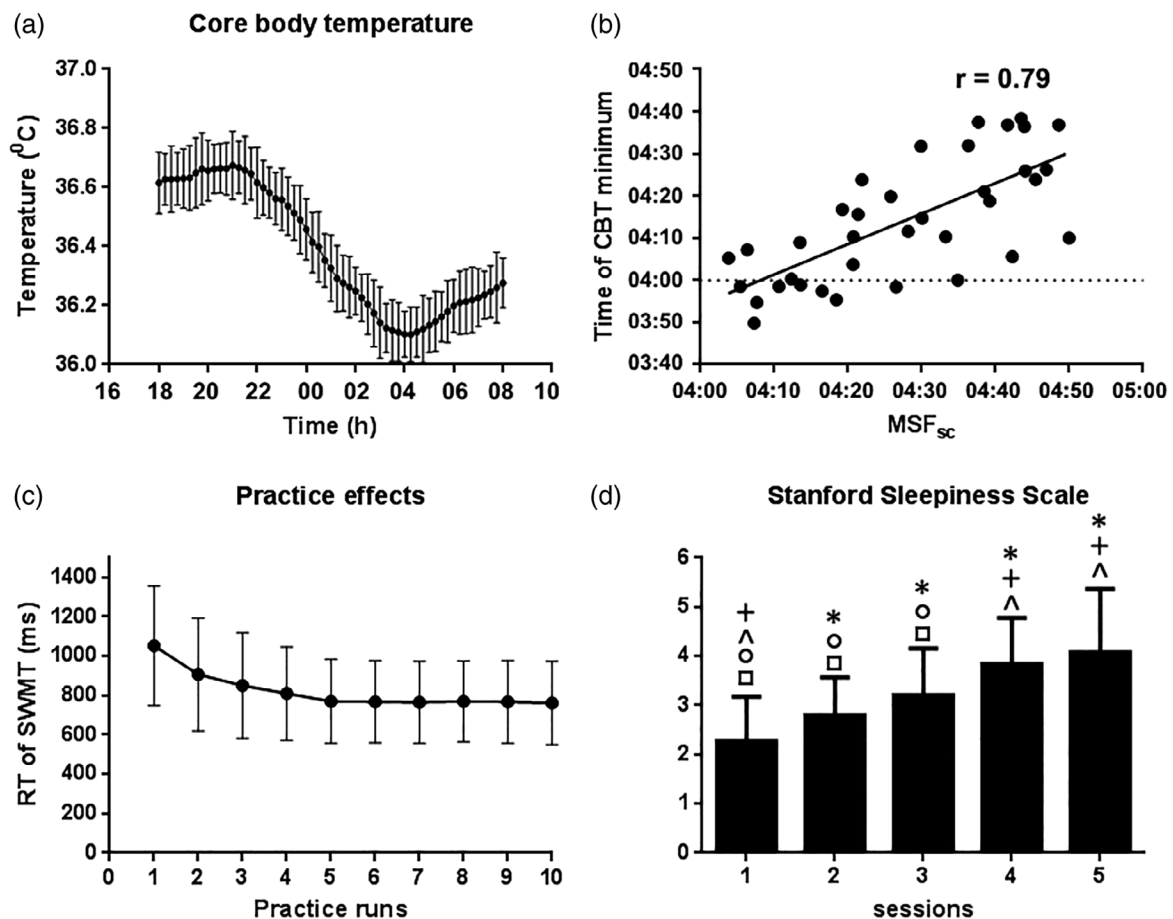


FIGURE 1 Figure 1a showed the raw core body temperature curves for the participants. Round symbols show 15-min averages with standard error bars. Figure 1b showed the correlation between individual MSF_{SC} and individual time of core body temperature minimum. Figure 1c Indicated the training effects for SWMT RT. repeated measures ANOVA showed significant training effects during the first five practices, the SWMT RT reached a stable level after five times of practice. Figure 1d indicated the behavioral results for the SSS. Repeated measures ANOVA showed a main effect of session for the SSS. Posthoc *t* tests were also performed to test for changes between sessions. * indicate a significant difference between the labeled session and Session 1 (e.g., Session 4 labeled by an asterisk indicates a significant difference in SSS between Sessions 4 and 1); + indicate a significant difference between the labeled session and Session 2; Δ indicate a significant difference between the labeled session and Session 3; ○ indicate a significant difference between the labeled session and Session 4; □ indicate a significant difference between the labeled session and Session 5. Abbreviation: MSF_{SC} , mid-sleep time on free days, corrected for sleep debt on work days

allowed to engage in nonstrenuous activities, such as watching videos and reading. Research assistants remained with the participants throughout the night to prevent them from falling asleep.

Core body temperature (CBT) is a reliable marker of endogenous circadian rhythmicity, and CBT minimum occurs at approximately the mid-point of sleep (Baehr, Revelle, & Eastman, 2000). Therefore, individual chronotypes were identified by the timing of the minimum CBT. From 6:00 p.m. on the first day to 8:00 a.m. on the second day, CBT was monitored continuously every 60 s using a wireless integrated physiological monitor (VitalSense[®], Mini Mitter, Bend, OR; Darwent, Zhou, Heuvel, Sargent, & Roach, 2011). The VitalSense[®] monitor receives radio signals from temperature-sensitive ingestible capsules with a sensing range of 25–50°C and generates a valid index of the CBT. The time of the CBT minimum was calculated using a previously described method by fitting a cosine function comprising the fundamental oscillation and its first harmonic (Taillard, Philip, Coste, Sagaspe, & Bioulac, 2003).

2.3 | Sternberg working-memory task

The SWMT used in this study was similar to a task that has been used in other imaging studies (Cui et al., 2015; Mu, Mishory, et al., 2005a). Stimuli were projected onto a screen using an LCD projector and viewed by participants through a mirror positioned above them on a head coil. The entire functional scan lasted for 12 min, 58 s, and consisted of an initial 10-s fixation cross followed by twelve 64-s stimulus blocks. Each block included a 32-s control task followed by a 32-s Sternberg task. Each task contained two 16-s trials. The control trial consisted of a 3-s viewing of six asterisks in two rows (2 × 3), followed by a 7-s delay and then a 3-s viewing of the word YES or NO presented at the center of the screen. Participants were asked to press the button corresponding to the word displayed on the screen and they were instructed to respond as fast as possible. During the WM trials, a row of 1, 3, or 6 randomized digits was presented on the screen. Participants viewed the set of digits for 3 s (encoding), and then maintained them memory during a 7-s delay period (retention) during which the screen was blank. Subsequently, a digit was presented on the screen for 3 s, and participants responded YES or NO according to whether the digit had been included in the initial digit set (recall). Each trial began and ended with a 1.5-s rest period. The RT was defined as the time from test-letter onset to the button response. The accuracy (percentage of correct trials) for a mean overall conditions (1 digit, 3 digit, and 6 digit) was also calculated for each participant in each session.

2.4 | MRI data acquisition

The imaging data were collected using a 3-Tesla MRI system (EXCITE; General Electric, Milwaukee, WI) at the Department of Radiology of Xijing Hospital, Fourth Military Medical University, Xi'an, China. Standard birdcage head coil and foam pads were used to minimize head motion and to diminish scanner noise. Functional images were obtained using a gradient-echo planar imaging (EPI) sequence with the following parameters: echo time

(TE) = 30 ms, repetition time (TR) = 2000 ms, data matrix = 64 × 64, field of view (FOV) = 240 mm × 240 mm, flip angle = 90°, and slices = 36. High-resolution, T1-weighted, three-dimensional (3D) anatomical data were also acquired using a 3D magnetization-prepared rapid gradient-echo sequence with the following parameters: TE = 3.18 ms, TR = 8.2 ms, data matrix = 256 × 256, FOV = 256 mm × 256 mm, flip angle = 9°, thickness = 1 mm, and slices with no gap = 196.

2.5 | MRI data analysis

Preprocessing and statistical analyses at individual and group levels were performed using Statistical Parametric Mapping software (SPM8; Wellcome Trust Centre for Neuroimaging, University College London, <http://www.fil.ion.ucl.ac.uk/spm>), implemented in MATLAB (MathWorks, Natick, MA). To eliminate the nonequilibrium effects of magnetization, the first five fMRI volumes were discarded. The remaining images were corrected for the acquisition delay between slices and then realigned to the first volume. Individual T1-weighted images were co-registered to the mean of the realigned functional echo-planar images. The Diffeomorphic Anatomical Registration through Exponentiated Lie Algebra (DARTEL) tool was used to compute the transformation from individual space to Montreal Neurological Institute (MNI) space (Ashburner, 2007). The fMRI images were normalized at a resolution of 3 × 3 × 3 mm³ using the same transformation information as the T1 images. These images were then smoothed with an 8-mm full-width-at-half-maximum isotropic Gaussian kernel.

A mixed-effects model was implemented using a two-stage process (first and second level). First-level analyses were modeled using the respective conditions (Sternberg task and control task) as regressors. The six head-motion parameters that were obtained during realignment were applied to take all head motion into account, and a high pass filter with a 128-s cutoff was used to remove effects related to low-frequency

TABLE 1 Demographic characteristics, mid-sleep times, and objective sleep measures

Males: N (%)	18 (50)
Age (years)	22.3 ± 1.7
Body mass index	23.4 ± 2.6
MCTQ questionnaire	
MSF _{SC}	04:26 ± 0:19
Objective sleep characteristics from actiwatch	
Time of falling asleep	00:06 ± 0:24
Number of wakening each night	27.3 ± 6.5
Sleep duration all night	6:44 ± 1:15
Sleep duration on nights before work days	6:26 ± 0:54
Sleep durations on nights before free days	7:03 ± 1:03
Sleep efficiency in %	83 ± 2.4
Sleep latency in minutes	15.6 ± 14.2

Values represent mean ± SEM (*n* = 36). Abbreviations: MCTQ, Munich Chronotype Questionnaire; MSF_{SC}, mid-sleep on free days, corrected for sleep debt on work days.

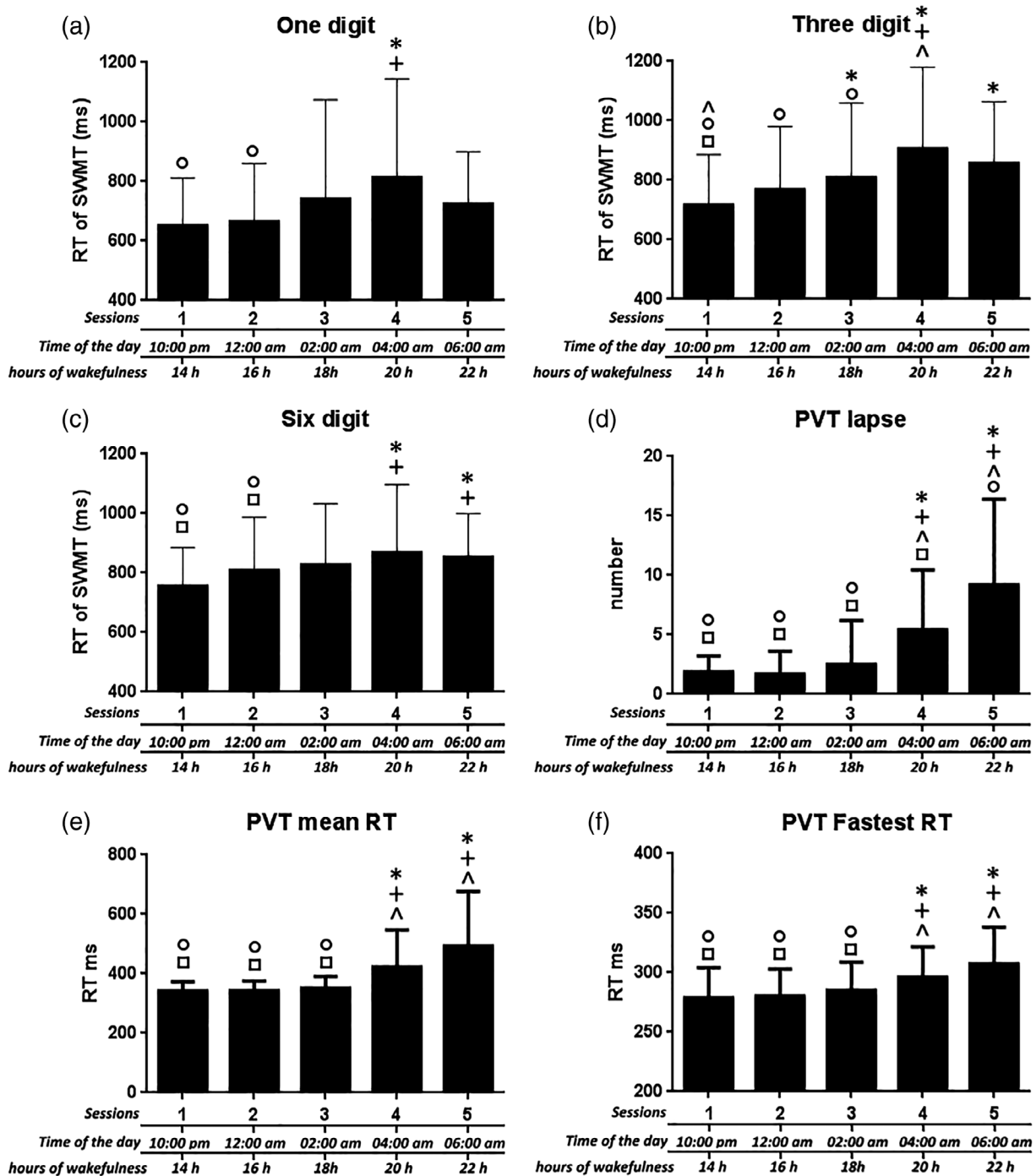


FIGURE 2 Behavioral results for the one-digit, three-digit, six-digit, and PVT lapse, PVT mean RT and PVT fastest RT. repeated measures ANOVA showed a main effect of session for these outcomes. Posthoc *t* tests were also performed to test for changes between sessions. * indicate a significant difference between the labeled session and Session 1; + indicate a significant difference between the labeled session and Session 2; ^ indicate a significant difference between the labeled session and Session 3; O indicate a significant difference between the labeled session and Session 4; □ indicate a significant difference between the labeled session and Session 5. Abbreviations: PVT, psychomotor vigilance task; RT, reaction time; SWMT, Sternberg working-memory task. The error bars represent standard deviations

changes such as heart beating. Contrast images between the Sternberg two task conditions were generated and then entered into a second-level model using the Sandwich Estimator method (SwE) to account for the within-subject correlation existing in our longitudinal data (Guillaume, et al., 2014). First, for each imaging session, a one-sample *t* contrast was

specified in the SwE contrast manager to examine the overall SWMT activation patterns. Second, an F contrast was specified in the SwE contrast manager to examine whether there were significant differences in SWMT activation patterns across sessions. Posthoc *t* comparison images between sessions were also calculated in the SwE contrast manager.

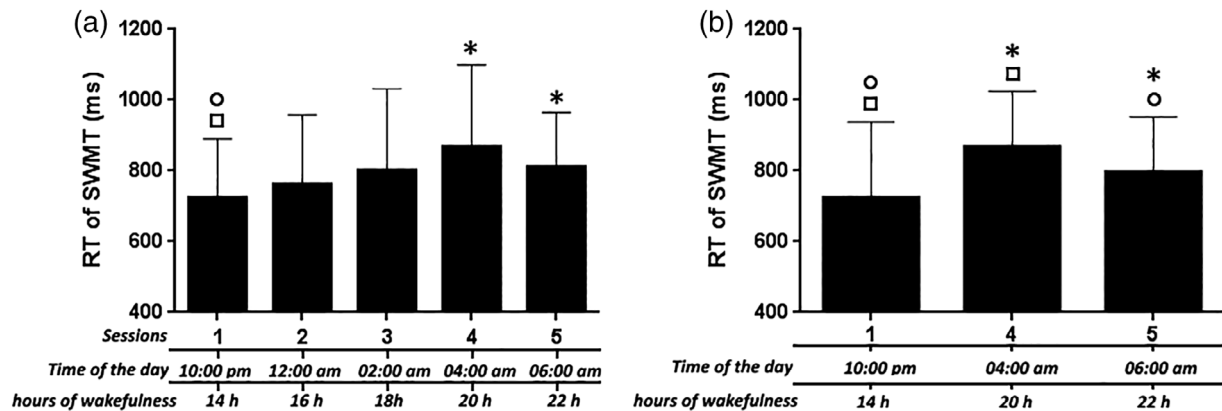


FIGURE 3 Behavioral results for RT of SWMT. Figure 3a indicated the results for all five sessions, Figure 3b indicated the results for three sessions (i.e., Sessions 1, 4, and 5). * indicate a significant difference between the labeled session and Session 1; ○ indicate a significant difference between the labeled session and Session 4; □ indicate a significant difference between the labeled session and Session 5. Abbreviations: RT, reaction time; SWMT, Sternberg working memory task. The error bars represent standard deviations

2.6 | Statistical inferences

Differences in mean RT were determined using a one-way repeated-measures ANOVA with an alpha of 0.05. Posthoc analysis used the Bonferroni–Holm method to correct for multiple comparisons between sessions (Holm, 1979). For other behavioral outcomes (accuracy, SSS, mean RT for 1, 3, and 6 digit sets, mean RT for the PVT, mean RT of the fastest PVT, and mean number of PVT lapses), one-way repeated-measures ANOVAs were carried out with an alpha of 0.01 to account for multiple comparisons. For posthoc comparisons, the alpha was set to 0.05 with Bonferroni correction. Correcting for multiple comparisons in the fMRI data analysis was accomplished using the false discovery rate (FDR) method (Guillaume, et al., 2014). For SWMT activation during different sessions, for F comparisons across different sessions, and for posthoc *t* comparisons between sessions, the statistical threshold was set to $p\text{FDR} < 0.05$. This corrected for multiple comparisons across the whole brain.

3 | RESULTS

Thirty-six participants successfully completed this study. All participants declared that they had not smoked or consumed any stimulants, medications, alcohol, or caffeine for at least 24 hr before scanning. General characteristics are shown in Table 1. CBT rhythms are plotted

in Figure 1a. The mean mid-sleep on free days, corrected for oversleep during the week (MSF_{SC}) obtained from Munich Chronotype Questionnaire (MCTQ) was 4:27 a.m. and the time of CBT minimum was 4:14 a.m.; significant positive correlations were found between MSF_{SC} and the time of CBT minimum (Figure 1b).

3.1 | Behavioral results

One-way repeated-measures ANOVA (rANOVA) revealed significant time effects for SSS (Figure 1d), mean RT for 1, 3, and 6 digit sets, mean RT for the PVT, mean RT of the fastest PVT, and mean number of PVT lapses (Figure 2). The rANOVA revealed that mean RT for the SWMT differed across sessions (Figure 3a; $F[4,140] = 7.02, p = 0.000$), and posthoc *t*-tests indicated significant differences between Sessions 1 and 4 ($p = 0.007$, Bonferroni corrected) and between Sessions 1 and 5 ($p = 0.048$). No other significant differences were found. Thus, only these three Sessions (1, 4, and 5) were evaluated in the following analysis. This rANOVA revealed a significant time effect (Figure 3b; $F[2,70] = 10.04, p = 0.000$), and posthoc tests indicated significant differences between Sessions 1 and 4 ($p = 0.002$), Sessions 1 and 5 ($p = 0.014$), and Sessions 4 and 5 ($p = 0.041$). A significant time effect was also found for the mean RT of Control (Table 2, $F[2,70] = 8.532, p = 0.000$), posthoc tests indicated significant differences between Sessions 1 and 4 ($p = 0.004$) and between Sessions 1 and 5 ($p = 0.002$). These results indicate that both the baseline performance and task

TABLE 2 Behavioral means (and standard deviations) for RT and accuracy of SWMT during sleep deprivation

	Session 1	Session 4	Session 5	P-value
Reaction time (ms)				
WM	724.58 (33.88)	866.85 (47.49)	801.32 (47.21)	0.0003
Control	571.15 (31.95)	673.19 (44.59)	657.91 (43.67)	0.0005
Accuracy (%)				
WM	93.40 (8.85)	90.97 (7.73)	91.62 (10.52)	0.47
Control	96.53 (4.86)	96.18 (6.49)	95.13 (6.91)	0.66

Values for WM represent a mean overall conditions (1 digit, 3 digit, and 6 digit), *p*-value indicated the one-way repeated-means ANOVAs carried out across three sessions.

performance were modulated by circadian and sleep-homeostatic factors. Interestingly, the accuracy for WM task trial and for Control trial showed no difference across the three sessions.

3.2 | Imaging results

3.2.1 | SWMT activation in different sessions

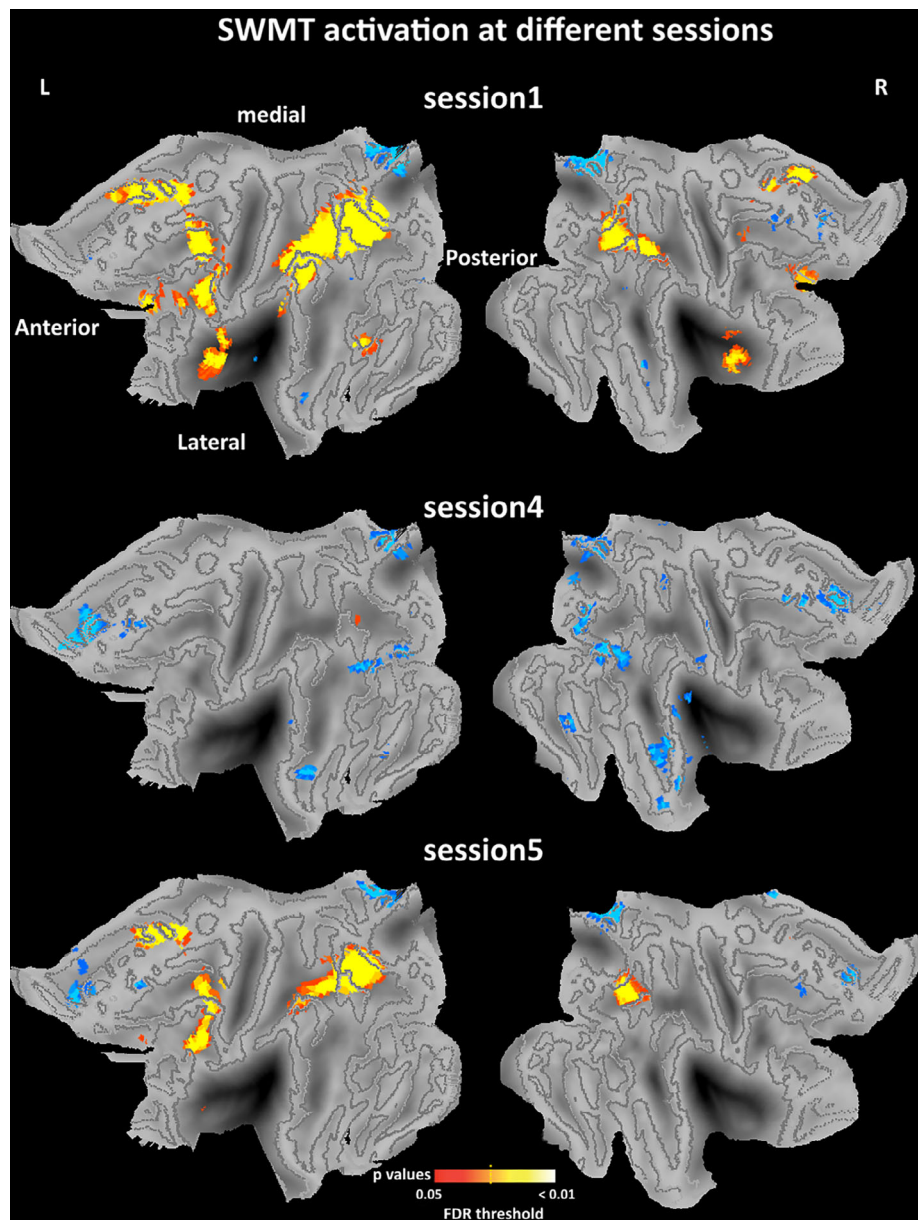
One-sample *t*-test results for brain activation during the three SWMT sessions are shown in Figure 4. Statistical maps were projected onto the flattened population-average landmark and surface-based atlases using CARET software (Van Essen, 2005). SWMT in Session 1 elicited extensive activation in brain regions related to cognitive control, such as the frontoparietal network and visual network, and some deactivation in brain regions within DMN. SWMT in Session 5 (6:00 a.m.) elicited little activation, indicating a pattern of decreased brain activation after a

whole night of TSD. However, SWMT in Session 4 (4:00 a.m.) elicited extensive deactivation in temporal, visual, and frontal lobes, and a small amount of activation in the parietal lobe. Thus as a whole, we did not observe a continuous decrease in activation during the night of TSD. In contrast, the SWMT in Session 4 was associated with the weakest activation (strongest deactivation), while SWMT activation in Session 5 had returned to a more active pattern that was characterized by increased activation in brain regions within the cognitive control network.

3.3 | ANOVA and posthoc results for the SWMT activation

To investigate significant changes in brain activation across the three sessions, one-way repeated ANOVA contrast was performed using the

FIGURE 4 One-sample imaging results for the SWMT in different sessions. One-sample *t* contrast was specified using the SwE contrast manager. The threshold was set at $pFDR < 0.05$ corrected for multiple comparisons. Statistical maps were projected onto the flattened left and right hemisphere of the population average landmark- and surface-based atlas in CARET software. Anterior, posterior, medial, and lateral directions are noted. Blue color refers to some deactivations in brain regions within default mode network. Abbreviation: SWMT, Sternberg working memory task [Color figure can be viewed at wileyonlinelibrary.com]



SwE method (FDR corrected). Posthoc contrasts were also performed using *t* tests to investigate the pairwise differences between sessions (FDR corrected). SWMT-specific activation is shown in Figure 5, Table 3, and Table 4. Activity in several regions changed significantly across sessions (ANOVA results), including the right superior frontal gyrus, right middle frontal gyrus, right medial frontal gyrus, right inferior frontal gyrus, right supplementary motor area, right inferior parietal gyrus, right precuneus, right putamen, bilateral supramarginal gyrus, bilateral insula, bilateral caudate and bilateral thalamus. Pairwise posthoc comparisons showed significant differences between Sessions 1 and 4, Sessions 1 and 5, and especially between Sessions 4 and 5 (Figure 5 and Table 4). The significant difference observed between Sessions 4 and 5 indicated a distinct increase in cerebral activation during the SWMT in the early morning of the TSD.

3.4 | Correlation of SWMT RT and cerebral activation

To investigate the functional relevance of these cerebral responses, we computed the correlations between RT during the SWMT and task-related cerebral responses in the three sessions. This was done in two steps: first, Conjunction analysis was used to calculate the overlapping brain regions across the three sessions, which are the regions that were activated (or deactivated) in all the three sessions. As shown in Figure 6a, overlapping regions of activation were found within the angular gyrus and overlapping regions of deactivation were found within the precuneus. For each participant, the mean parameter estimate obtained in the first-level statistical analysis for each area (angular gyrus and precuneus) in each session was computed and correlated with the respective SWMT RT. Figure 6b shows the correlation results. For the precuneus, no significant correlations were found between SWMT RT and the mean parameter estimate in any session. For the angular gyrus, significant negative correlations were found between SWMT RT and the mean parameter estimate in Session 4 ($r = -0.58, p < 0.001$, blue line in Figure 6b), meaning that stronger activity in the angular gyrus was associated with shorter RT during the SWMT task. A significant negative correlation was also found when analyzing all three sessions together ($r = -0.41, p < 0.001$, black line in Figure 6b). No significant correlations were found in Session 1 or Session 5.

The second step was to investigate how the interactions between functional brain networks were related to the SWMT RT. As shown in Figures 4 and 5, increased brain activity was mainly found within the cognitive control network and decreased brain activity was mainly found in the DMN. Anti-correlation between these two networks might be part of the neural basis underlying SWMT RT during TSD. Recent reports have indicated that each sub-network making up a certain functional network has a specialty (Yeo et al., 2011). Therefore, we sought to find sub-networks within the 17-region network described by a recent study that were the most representative of our findings (Yeo et al., 2011). The 17-network parcellation of the cerebral cortex were brought up by Yeo, Tandi, and Chee (2015). The 17 networks were divided into eight groups (Default, Control, Limbic, Salience/Ventral Attention, Dorsal Attention, Somatomotor, Visual, and TempPar), which broadly correspond to major networks discussed in the literature. The 17 networks are referred to as

“Default A,” “Default B,” and so on. The Default A is the “core” sub-network of DMN which comprises posterior cingulate cortex (PCC) and medial prefrontal cortex (mPFC), The Control A is sub-network of frontal-parietal control network which comprises dorsal PFC, lateral

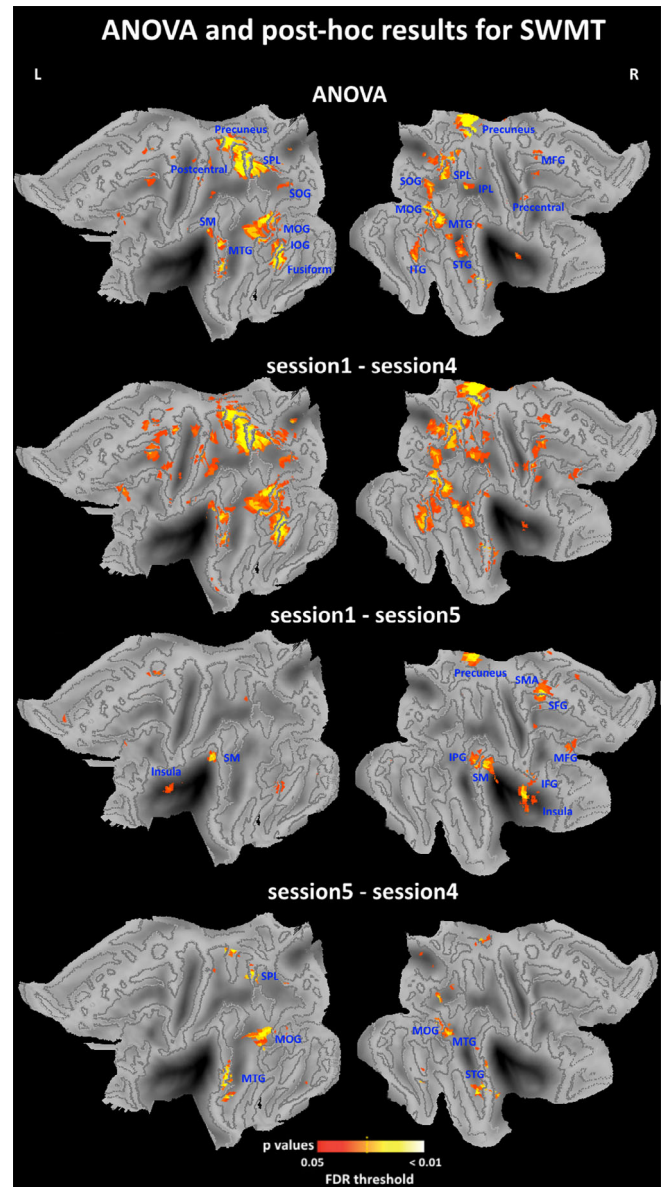


FIGURE 5 ANOVA and posthoc imaging results for the SWMT. *F* contrast and posthoc *t* contrast were specified in the SwE contrast manager. The threshold was set at $p\text{FDR} < 0.05$ corrected for multiple comparisons. Statistical maps were projected onto the flattened left and right hemisphere of the population average landmark- and surface-based atlas in CARET software. Abbreviations: IFG, inferior frontal gyrus; IOG, inferior occipital gyrus; IPL, inferior parietal lobule; ITG, inferior temporal gyrus; L, left; MFG, medial frontal gyrus; MOG, middle occipital gyrus; MTG, middle temporal gyrus; R, right; SFG, Superior frontal gyrus; SM, supramarginal gyrus; SMA, supplementary motor area; SOG, superior occipital gyrus; SPL, superior parietal lobule; STG, superior temporal gyrus; SWMT, Sternberg working-memory task [Color figure can be viewed at wileyonlinelibrary.com]

PFC, ventro-lateral PFC, anterior cingulate cortex, intraparietalsulcus (IPS), and temporal lobe. As shown in Figure 7, the sub-networks Control A and Default A are the closest to our findings, and we thus selected them to investigate the functional relevance of their interactions. Using the aforementioned Default A network and Control A network as masks, the time-course of each mask for each participant was obtained. For each participant, the time-courses of control A and default A in each session were computed and anti-correlations during each session were then assessed by computing pair-wise correlations between the time-courses of control A and default A. We removed the effects of spurious signal variations, including head-movement parameters, average signals in the ventricles, and white matter and whole-brain global signals before computing the correlations between time-courses, by means of linear regression (Lei, Wang, Yuan, & Mantini, 2014). The individual anti-correlation in each session was then correlated with their respective SWMT RTs. An rANOVA for the three sessions revealed significant that anti-correlations between control A and default A differed significantly across sessions (Figure 6c; $F[2,70] = 8.78, p = 0.000$). Posthoc tests indicated significant differences between Sessions 1 and 4 ($p = 0.007$), Sessions 1 and 5 ($p = 0.026$), and Sessions 4 and 5 ($p = 0.039$). Significant positive correlations were found between SWMT RT and the anti-correlations in Session 4 (Figure 6d, blue line; $r = 0.54, p < 0.001$). A significant positive correlation was also found when combining the three sessions together (Figure 6d, black line; $r = 0.37, p < 0.001$). No significant correlations were found between Session 1 and Session 5.

4 | DISCUSSION

The present study investigated dynamic changes in SWMT performance and the accompanying cerebral responses by obtaining repeated fMRI measurements during one night of TSD. Unlike the PVT outcomes that showed gradual deteriorations, RTs for the SWMT in participants with intermediate chronotypes improved in Session 5 (6:00 a.m.) compared with Session 4 (4:00 a.m.). Cerebral responses during the SWMT showed distinct differences across the three sessions, indicating a clear modulation of circadian rhythm and homeostatic sleep pressure on WM brain responses. Finally, RTs for the SWMT were found to be strongly correlated with task-related activation in the angular gyrus and with the degree of negative correlation between the control and default networks.

In this study, only participants with intermediate chronotypes were recruited. Chronotype-specificity refers to individual preferences in sleep and wakefulness that reflect endogenous, self-sustained genetic dispositions (Roenneberg & Merrow, 2016). Chronotypes have been found to be associated with differences in white matter integrity and gray matter density (Rosenberg, Maximov, Reske, Grinberg, & Shah, 2014; Takeuchi et al., 2015). Additionally, chronotype-specific cerebral responses to language processing and attention also have been found (Reske, Rosenberg, Plapp, Kellermann, & Shah, 2015; Rosenberg, Reske, Warbrick, & Shah, 2015). Those findings highlight the importance of considering sleep preferences in neuroimaging studies. Most importantly,

TABLE 3 Peak coordinates of significant brain regions in ANOVA results for the activation of SWMT

Regions-(ANOVA)	Number of voxels	Peak coordinates (MNI)			F-value
		x	y	z	
Right precentral gyrus	37	51	3	48	9.4
Right middle frontal gyrus	30	27	39	14	10.4
Left superior occipital gyrus	47	-24	-75	24	12.7
Right superior occipital gyrus	91	21	-66	48	11.9
Left middle occipital gyrus	177	-45	-75	18	12.1
Right middle occipital gyrus	152	39	-69	18	14.3
Left inferior occipital gyrus	76	-45	-60	-12	12.1
Left fusiform	77	-42	-60	-15	13.7
Left postcentral gyrus	45	-24	-36	66	10.8
Left superior parietal gyrus	222	-24	-60	57	17.6
Right superior parietal gyrus	101	18	-66	51	12.4
Right inferior parietal gyrus	46	27	-48	51	12.9
Left supramarginal gyrus	35	-54	-42	33	10.6
Left precuneus	149	-12	-57	66	13.9
Right precuneus	156	12	-42	54	14.7
Right superior temporal gyrus	35	54	3	-12	11.2
Left middle temporal gyrus	198	-63	-24	0	11.1
Right middle temporal gyrus	247	39	-66	18	13.4
Right inferior temporal gyrus	52	51	-72	-3	9.8

Significance was set at $p < 0.05$ (false discovery rate corrected).

TABLE 4 Peak coordinates of significant brain regions in posthoc results for the activation of SWMT

Regions-(S1–S5)	Number of voxels	Peak coordinates (MNI)			t-value
		x	y	z	
Right superior frontal gyrus	53	18	3	72	5.5
Right middle frontal gyrus	105	39	45	36	5.5
Right inferior frontal gyrus	34	39	9	15	6.5
Right supplemental motor area	102	15	3	72	5.4
Left insula	30	–30	18	12	4.9
Right insula	120	36	9	15	6.2
Right inferior parietal gyrus	42	57	–48	51	4.9
Left supramarginal gyrus	50	–54	–42	33	6.1
Right supramarginal gyrus	189	66	–36	36	5.7
Right precuneus	44	15	–45	51	6.3
Left caudate	94	–21	6	21	6.8
Right caudate	88	18	–6	21	5.9
Right putamen	73	27	18	9	5.6
Left thalamus	90	–9	–9	18	5.2
Right thalamus	74	15	–9	18	5.4

Regions-(S5–S4)	Number of voxels	Peak coordinates (MNI)			t-value
		x	y	z	
Left middle occipital gyrus	53	–48	–75	15	5.8
Right middle occipital gyrus	32	45	–81	18	5.7
Left superior parietal gyrus	35	–24	–60	57	6.1
Right superior temporal gyrus	40	54	3	–12	5.9
Left middle temporal gyrus	144	–63	–27	0	5.9
Right middle temporal gyrus	110	48	3	–27	5.8

Significance was set at $p < 0.05$ (false discovery rate corrected).

participants with different chronotypes have different optimal times of day (maximal circadian wake promotion), which are generally 10–12 hr after each individual wakes up. As participants with morning chronotypes sleep early and wake up early while participants with evening chronotypes sleep late and wake up late, when behavioral tasks are administered at a certain time of night, the observed cerebral responses might be contaminated by the individual differences in chronotype. Therefore, we only recruited participants with intermediate chronotypes, and further verified the MSF_{SC} obtained from the MCTQ using the time of CBT minimum.

Performance on the PVT deteriorated monotonically over time while the RT of the SMWT showed a biphasic curve with an early gradual deterioration before Session 4 and later recovery in Session 5. This is consistent with current literature indicating that different cognitive tasks are differentially affected by sleep loss and circadian rhythmicity (Lo et al., 2012). The finding that the slowest RT of the SWMT occurred at 4:00 a.m. is consistent with a previous study in which the maximum effects of circadian rhythmicity and sleep history on *n*-back WM were found to be at around 4 hr DLMO, which, in that study, corresponded to 4:00 a.m. of clock time (Chen et al., 2015). In particular, for participants with the clock gene $PER3^{4/5}$ heterozygotes,

the performance on 3-back WM was also found to be improved after 4:00 a.m. (Guillaume et al., 2014). Previous studies have shown that the chronotype of participants with heterozygous $PER3^{4/5}$ are more likely to show an intermediate chronotype (Dijk & Archer, 2010; Lázár et al., 2012), their habitual bedtime, wake time, and MSF_{SC} recorded by actigraphy are located between the two homozygous versions of PER ($PER3^{4/4}$ and $PER3^{5/5}$), and were largely consistent with our results for participants with intermediate chronotypes (Table 1). Collectively, this evidence supports our findings that WM performance during TSD in participants with intermediate chronotype showed an improvement after the morning hours at around the mid-time point of their regular biological night.

We also investigated the cerebral responses underlying the dynamic characteristics of SWMT RT. During Session 1 (10:00 p.m.) and Session 5 (6:00 a.m.) we identified bilateral frontal–parietal network of WM similar to that observed in previous studies after RW and TSD, respectively (Chee & Choo, 2004; Cui et al., 2015; Mu et al., 2005b; Reichert et al., 2016). In keeping with the existing literature (Choo, Lee, Venkatraman, Sheu, & Chee, 2005; Lythe et al., 2012), significant differences between Sessions 1 and 5 were primarily found in the frontoparietal and attentional networks, which included frontal

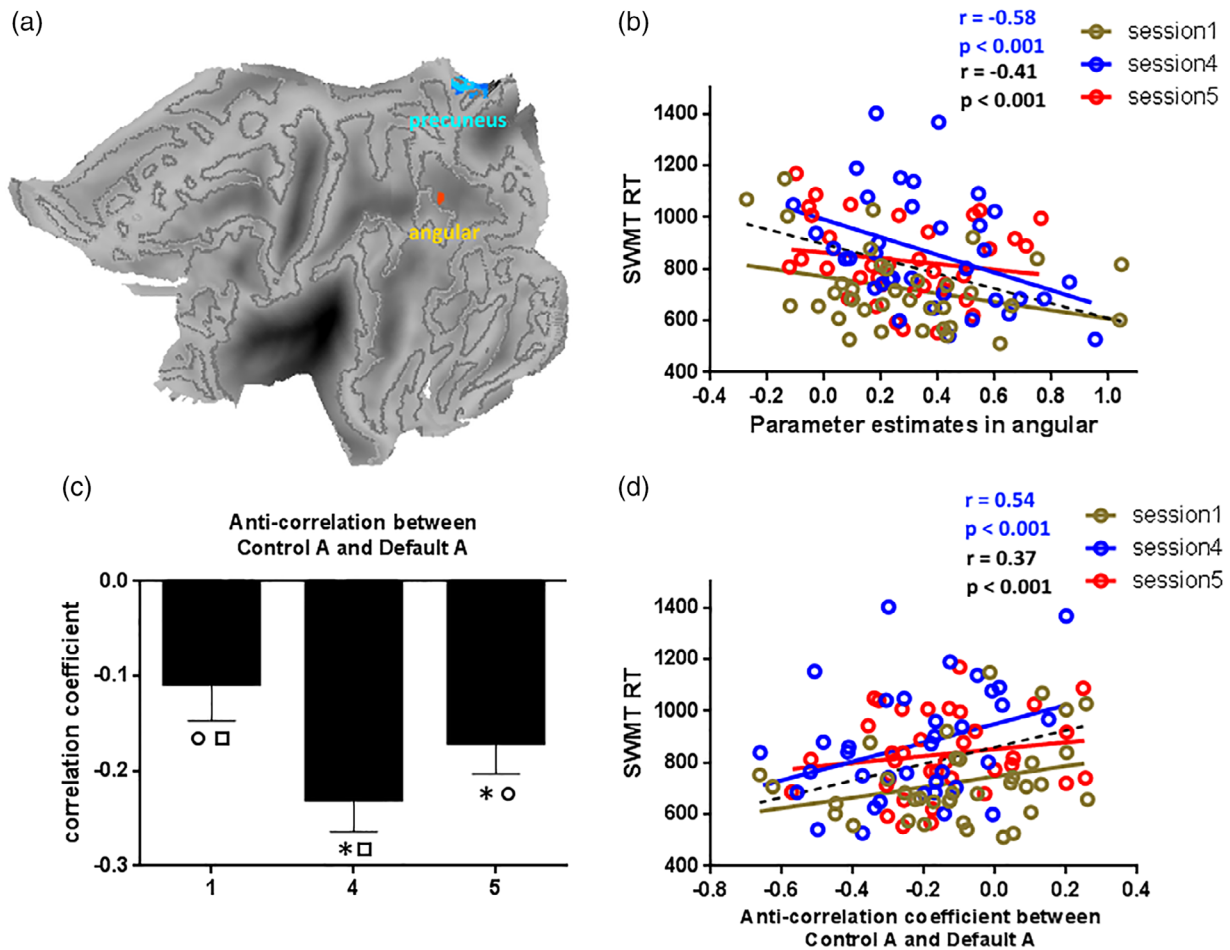


FIGURE 6 Correlation results for RT of SWMT. Figure 5a indicated the overlapping regions for one-sample imaging results in different sessions. Figure 5b indicated the correlation results between the parameter estimates in angular and SWMT RT in three sessions, the correlation result was only significant in Session 4. Figure 5c indicated the ANOVA result for anti-correlation between control A and default A. Figure 5d indicated the correlation results between the anti-correlation coefficient and SWMT RT in three sessions, the correlation result was only significant in Session 4. * indicate a significant difference between the labeled session and Session 1; ○ indicate a significant difference between the labeled session and Session 4; □ indicate a significant difference between the labeled session and Session 5. Abbreviations: RT, reaction time; SWMT, Sternberg working memory task [Color figure can be viewed at wileyonlinelibrary.com]

(superior, middle, and inferior frontal gyrus), parietal (inferior parietal gyrus, supplementary motor area, and supramarginal gyrus), and sub-cortical areas (caudate, putamen, and thalamus). However, activation patterns in Session 4 showed distinguishing cerebral responses characterized by extensive deactivation and little activation. Most importantly, the deactivation was not confined within the DMN, but also occurred within higher-order brain regions. This suggested a nearly unresponsive pattern during Session 4. Among these three sessions, the slowest SWMT RT and weakest cerebral responses were found during the early morning (4:00 a.m.) hours of the TSD. Therefore, previous studies missed critical information because the typical TSD condition occurs after the rebound of SWMT performance and the rebound of SWMT activation. These findings also provided evidence supporting the idea that simple tasks (such as the PVT) were more affected by TSD than complex tasks (such as the SWMT task; Balkin et al., 2004; Lim & Dinges, 2010). As indicated by a recent study (Muto et al., 2016), cerebral responses during PVT in higher-order

frontal, parietal, visual, and sensorimotor cortices gradually decreased during TSD. Therefore, the differential effects of TSD on brain activity related to complex and simple cognitive tasks might depend on the typical circadian phase at which performance is assessed.

Significant negative correlations were found between SWMT RT and activation in the overlapping angular gyrus, which was also the only region activated by the task during Session 4. This unique activation and the significant correlation suggest that although Session 4 was characterized by low levels of activity and poor task performance, the angular gyrus stands an important role in supporting the remaining ability for WM. However, reduced activity within the precuneus showed no significant correlations, suggesting that task-related suppression of activity in the DMN alone was not associated the SWMT RT (Kelly, Uddin, Biswal, Castellanos, & Milham, 2008; Lei et al., 2014), the competitive relationship between the default and control networks, as found in our study, might underlie SWMT performance during TSD. The time of session significantly affected the anti-

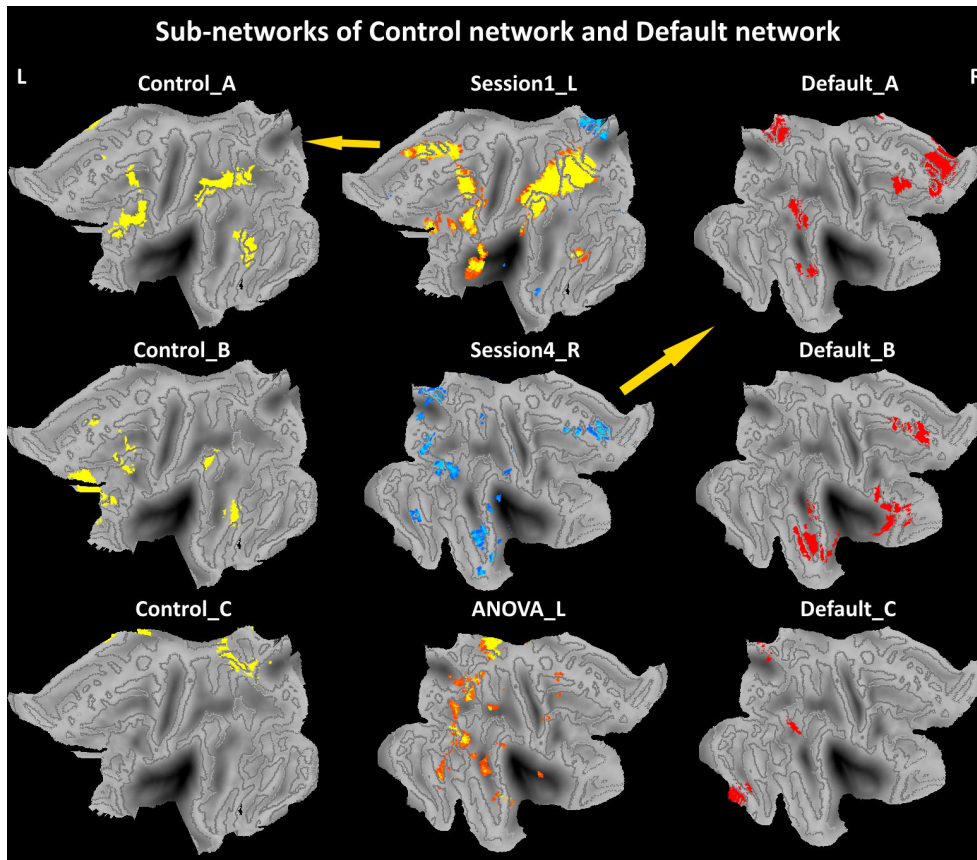


FIGURE 7 Sub-networks of control network and default network. Those maps were projected onto the flattened left hemisphere of the population average landmark- and surface-based atlas in CARET software. Abbreviations: L, left; R, right [Color figure can be viewed at wileyonlinelibrary.com]

correlations between control and default sub-networks, which suggests that circadian rhythm and homeostatic sleep pressure can modulate interactions between functional networks. This finding was consistent with a recent study in which the intrinsic connectivity pattern of two DMN sub-networks was clearly modulated by daily rhythms (Blautzik et al., 2013). However, in the current study, the correlations were only evident during Session 4, while neither positive nor negative correlations reached significance during Session 1 or Session 5. This supports the idea that the surviving activity in the angular gyrus and interactions between the control and default networks are functionally significant in maintaining performance during the worst period of TSD. Because the activation patterns during relatively normal periods were characterized by widespread activation, maintaining performance during these periods might not rely solely on these two cerebral mechanisms. One limitation of our current study is that we did not set a control condition in which participants did not accumulate sleep debt (using nap technique). The comparison between the sleep deprived and nonsleep deprived conditions could be a direct way to know the effect of sleep deprivation.

To conclude, by increasing the number of fMRI examinations during TSD, we were able to investigate the dynamic changes in SWMT RT and the underlying cerebral responses during one night of TSD. The clear rebound of performance and response found in our study constitutes direct evidence for the fact that different cognitive task was differentially modulated by interactions between homeostatic sleep pressure and circadian rhythmicity. It is therefore important to

consider the circadian phase at which performance is assessed when investigating the effects of TSD on cognitive function and brain activity. However, it is important to note that all studies investigating cerebral responses (and/or cognitive performance) during TSD cannot disentangle sleep homeostatic and circadian effects but can only investigate the impact of the interaction of these two processes. To disentangle circadian from sleep homeostatic effects, forced desynchrony studies are further needed to be conducted.

ACKNOWLEDGMENT

The authors would like to thank Ting Zhou for assistance with data collection. This study was financially supported by National Basic Research Program of China under Grant No. 2015CB856403, the National Natural Science Foundation of China under Grant Nos. 81571651, 81601474, and 81801772.

CONFLICT OF INTEREST

This was not an industry supported study. The authors have indicated no financial conflict of interest.

ORCID

Yuanqiang Zhu  <https://orcid.org/0000-0001-7685-1539>

REFERENCES

- Ashburner, J. (2007). A fast diffeomorphic image registration algorithm. *NeuroImage*, 38, 95–113.
- Baehr, E. K., Revelle, W., & Eastman, C. I. (2000). Individual differences in the phase and amplitude of the human circadian temperature rhythm: With an emphasis on morningness–eveningness. *Journal of Sleep Research*, 9, 117–127.
- Balkin, T. J., Bliese, P. D., Belenky, G., Sing, H., Thorne, D. R., Thomas, M., ... Wesensten, N. J. (2004). Comparative utility of instruments for monitoring sleepiness-related performance decrements in the operational environment. *Journal of Sleep Research*, 13, 219–227.
- Basner, M., Rao, H., Goel, N., & Dinges, D. F. (2013). Sleep deprivation and neurobehavioral dynamics. *Current Opinion in Neurobiology*, 23, 854–863.
- Blautzik, J., Vetter, C., Peres, I., Gutyrchik, E., Keeser, D., Berman, A., ... Reiser, M. (2013). Classifying fMRI-derived resting-state connectivity patterns according to their daily rhythmicity. *NeuroImage*, 71, 298–306.
- Chee, M. W. L., & Choo, C. W. (2004). Functional imaging of working memory after 24 hr of total sleep deprivation. *The Journal of Neuroscience*, 24, 4560–4567.
- Chee, M. W. L., Chuah, L. Y. M., Venkatraman, V., Chan, W. Y., Philip, P., & Dinges, D. F. (2006). Functional imaging of working memory following normal sleep and after 24 and 35 h of sleep deprivation: Correlations of fronto-parietal activation with performance. *NeuroImage*, 31, 419–428.
- Chen, Q., Yang, H., Zhou, N., Sun, L., Bao, H., Tan, L., ... Huang, L. (2015). Inverse U-shaped association between sleep duration and semen quality: Longitudinal observational study (MARHCS) in Chongqing, China. *Sleep*, 39, 79–86.
- Choo, W. C., Lee, W. W., Venkatraman, V., Sheu, F. S., & Chee, M. W. L. (2005). Dissociation of cortical regions modulated by both working memory load and sleep deprivation and by sleep deprivation alone. *NeuroImage*, 25, 579–587.
- Cui, J., Tkachenko, O., Gogel, H., Kipman, M., Preer, L. A., Weber, M., ... Buchholz, J. L. (2015). Microstructure of frontoparietal connections predicts individual resistance to sleep deprivation. *NeuroImage*, 106, 123–133.
- Darwent, D., Zhou, X., Heuvel, C.v.d., Sargent, C., & Roach, G. D. (2011). The validity of temperature-sensitive ingestible capsules for measuring core body temperature in laboratory protocols. *Chronobiology International*, 28, 719–726.
- Dijk, D.-J., & Archer, S. N. (2010). PERIOD3, circadian phenotypes, and sleep homeostasis. *Sleep Medicine Reviews*, 14, 151–160.
- Durmer, J. S., & Dinges, D. F. (2005). Neurocognitive consequences of sleep deprivation. *Seminars in Neurology*, 25, 117–129.
- Goel, N., Rao, H., Durmer, J. S., & Dinges, D. F. (2009). Neurocognitive consequences of sleep deprivation. *Seminars in Neurology*, 29, 320–339.
- Guillaume, B., Hua, X., Thompson, P. M., Waldorp, L., Nichols, T. E., & Alzheimer's Disease Neuroimaging Initiative. (2014). Fast and accurate modelling of longitudinal and repeated measures neuroimaging data. *NeuroImage*, 94, 287–302.
- Habeck, C., Rakitin, B. C., Moeller, J., Scarmeas, N., Zarahn, E., Brown, T., & Stern, Y. (2004). An event-related fMRI study of the neurobehavioral impact of sleep deprivation on performance of a delayed-match-to-sample task. *Brain Research. Cognitive Brain Research*, 18, 306–321.
- Holm, S. (1979). A simple sequentially rejective multiple test procedure. *Scandinavian Journal of Statistics*, 6, 65–70.
- Kelly, A. C., Uddin, L. Q., Biswal, B. B., Castellanos, F. X., & Milham, M. P. (2008). Competition between functional brain networks mediates behavioral variability. *NeuroImage*, 39, 527–537.
- Klerman, E. B., Gershengorn, H. B., Duffy, J. F., & Kronauer, R. E. (2002). Comparisons of the variability of three markers of the human circadian pacemaker. *Journal of Biological Rhythms*, 17, 181–193.
- Lázár, A. S., Slak, A., Lo, J. C.-Y., Santhi, N., von Schantz, M., Archer, S. N., ... Dijk, D.-J. (2012). Sleep, diurnal preference, health, and psychological well-being: A prospective single-allelic-variation study. *Chronobiology International*, 29, 131–146.
- Lei, X., Wang, Y., Yuan, H., & Mantini, D. (2014). Neuronal oscillations and functional interactions between resting state networks. *Human Brain Mapping*, 35, 3517–3528.
- Lim, J., & Dinges, D. F. (2010). A meta-analysis of the impact of short-term sleep deprivation on cognitive variables. *Psychological Bulletin*, 136, 375–389.
- Lo, J. C., Groeger, J. A., Santhi, N., Arbon, E. L., Lazar, A. S., Hasan, S., ... Dijk, D.-J. (2012). Effects of partial and acute total sleep deprivation on performance across cognitive domains, individuals and circadian phase. *PLoS One*, 7, e45987.
- Lythe, K. E., Williams, S. C. R., Anderson, C., Libri, V., & Mehta, M. A. (2012). Frontal and parietal activity after sleep deprivation is dependent on task difficulty and can be predicted by the fMRI response after normal sleep. *Behavioural Brain Research*, 233, 62–70.
- Mu, Q., Mishory, A., Johnson, K. A., Nahas, Z., Kozel, F. A., Yamanaka, K., ... George, M. S. (2005a). Decreased brain activation during a working memory task at rested baseline is associated with vulnerability to sleep deprivation. *Sleep*, 28, 433–446.
- Mu, Q., Nahas, Z., Johnson, K. A., Yamanaka, K., Mishory, A., Koola, J., ... George, M. S. (2005b). Decreased cortical response to verbal working memory following sleep deprivation. *Sleep*, 28, 55–67.
- Muto, V., Jaspas, M., Meyer, C., Kussé, C., Chellappa, S. L., Degueldre, C., ... Middleton, B. (2016). Local modulation of human brain responses by circadian rhythmicity and sleep debt. *Science*, 353, 687–690.
- Reichert, C. F., Maire, M., Schmidt, C., & Cajochen, C. (2016). Sleep-wake regulation and its impact on working memory performance: The role of adenosine. *Biology*, 5, 11.
- Reske, M., Rosenberg, J., Plapp, S., Kellermann, T., & Shah, N. J. (2015). fMRI identifies chronotype-specific brain activation associated with attention to motion—Why we need to know when subjects go to bed. *NeuroImage*, 111, 602–610.
- Roenneberg, T., & Merrow, M. (2016). The circadian clock and human health. *Current Biology*, 26, R432–R443.
- Roenneberg, T., Wirz-Justice, A., & Merrow, M. (2003). Life between clocks: Daily temporal patterns of human chronotypes. *Journal of Biological Rhythms*, 18, 80–90.
- Rosenberg, J., Maximov, I. I., Reske, M., Grinberg, F., & Shah, N. J. (2014). “Early to bed, early to rise”: Diffusion tensor imaging identifies chronotype-specificity. *NeuroImage*, 84, 428–434.
- Rosenberg, J., Reske, M., Warbrick, T., & Shah, N. (2015). Chronotype modulates language processing-related cerebral activity during functional MRI (fMRI). *PLoS One*, 10, e0137197.
- Sateia, M. J. (2014). International classification of sleep disorders-third edition. *Chest*, 146, 1387–1394.
- Schmidt, C., Fabienne, C., Christian, C., & Philippe, P. (2007). A time to think: Circadian rhythms in human cognition. *Cognitive Neuropsychology*, 24, 755–789.
- Taillard, J., Philip, P., Coste, O., Sagaspe, P., & Bioulac, B. (2003). The circadian and homeostatic modulation of sleep pressure during wakefulness differs between morning and evening chronotypes. *Journal of Sleep Research*, 12, 275–282.
- Takeuchi, H., Taki, Y., Sekiguchi, A., Nouchi, R., Kotozaki, Y., Nakagawa, S., ... Shinada, T. (2015). Regional gray matter density is associated with morningness–eveningness: Evidence from voxel-based morphometry. *NeuroImage*, 117, 294–304.
- Van Essen, D. C. (2005). A population-average, landmark-and surface-based (PALS) atlas of human cerebral cortex. *NeuroImage*, 28, 635–662.
- Xu, J., Zhu, Y., Fu, C., Sun, J., Li, H., Yang, X., ... Tian, J. (2015). Frontal metabolic activity contributes to individual differences in vulnerability toward total sleep deprivation-induced changes in cognitive function. *Journal of Sleep Research*, 25(2), 169–180.

- Yeo, B. T., Krienen, F. M., Sepulcre, J., Sabuncu, M. R., Lashkari, D., Hollinshead, M., ... Polimeni, J. R. (2011). The organization of the human cerebral cortex estimated by intrinsic functional connectivity. *Journal of Neurophysiology*, *106*, 1125–1165.
- Yeo, B. T., Tandi, J., & Chee, M. W. (2015). Functional connectivity during rested wakefulness predicts vulnerability to sleep deprivation. *NeuroImage*, *111*, 147–158.
- Zhu, Y., Feng, Z., Xu, J., Fu, C., Sun, J., Yang, X., ... Qin, W. (2015). Increased interhemispheric resting-state functional connectivity after sleep deprivation: A resting-state fMRI study. *Brain Imaging and Behavior*, *10*(3), 911–919.
- Zhu, Y., Xi, Y., Fei, N., Liu, Y., Zhang, X., Liu, L., ... Yin, H. (2017). Dynamics of cerebral responses to sustained attention performance during one night of sleep deprivation. *Journal of Sleep Research*, *27*(2), 184–196.

How to cite this article: Zhu Y, Xi Y, Sun J, et al. Neural correlates of dynamic changes in working memory performance during one night of sleep deprivation. *Hum Brain Mapp.* 2019;40: 3265–3278. <https://doi.org/10.1002/hbm.24596>